Journal of Materials Chemistry B

ROYAL SOCIETY OF CHEMISTRY

PAPER

View Article Online
View Journal | View Issue

Cite this: J. Mater. Chem. B, 2025, 13, 10609

Taraxacum mongolicum Hand.-Mazz. derived extracellular vesicles alleviate mastitis *via* NLRP3 inflammasome and NF-κB/MAPK pathways†

Yuan Sun,[a] Ying Liu,[a] Jinxian Li,[a] Shan Huang,[b] Yiyang Du,[a] Danyang Chen,[a] Min Yang*[a] and Yinghua Peng *[a]

Received 12th April 2025,
Accepted 16th July 2025

DOI: 10.1039/d5tb00861a

rsc.li/materials-b

Mastitis, a prevalent inflammatory disease affecting both humans and animals, imposes significant health burdens globally. *Taraxacum mongolicum* Hand.-Mazz. has been traditionally used to treat mammary gland disorders, however, the clinical translation of its crude extracts remains challenging due to the poor bioavailability. Emerging as innovative nanotherapeutic agents, plant-derived extracellular vesicles (PEVs) exhibit enhanced bioavailability, low immunogenicity, and targeted delivery capabilities, making them promising candidates for precision medicine applications. Herein, extracellular vesicles derived from *Taraxacum mongolicum* Hand.-Mazz. (TH-EVs) were successfully isolated employing ultracentrifugation and sucrose gradient centrifugation. Subsequently, these physicochemical properties, including particle size distribution and composition analysis, were comprehensively characterized. The anti-inflammatory efficacy and mechanism of TH-EVs were explored in both lipopolysaccharide (LPS)-stimulated murine mammary epithelial cells (HC11) and a murine mastitis model. *In vitro*, TH-EVs reduced TNF-α, IL-6, IL-1β and cellular oxidative stress. *In vivo*, TH-EVs alleviated histopathological damage, decreased myeloperoxidase activity, inhibited T lymphocyte activation, and reduced oxidative stress in mammary tissues. Mechanistically, TH-EVs inhibited the NLRP3 inflammasome, NF-κB and MAPK pathways. This study demonstrates that TH-EVs are a potent natural nanotherapeutic agent for mastitis, with potential for translational applications.

1. Introduction

Mastitis, an inflammatory disorder of the mammary gland, predominantly affects humans and livestock, with dairy cows being particularly vulnerable.[1] In lactating women, this condition complicates 3%–20% of breastfeeding cases, often leading to psychological distress and premature weaning.[2–4] The global dairy industry suffers huge losses every year due to bovine mastitis-induced milk quality deterioration and production decline.[5,6] Gram-negative bacterial pathogens, particularly through lipopolysaccharide (LPS)-mediated inflammatory cascades, drive disease pathogenesis in both clinical scenarios.[7,8] While antibiotics remain the therapeutic mainstay, escalating antimicrobial resistance (AMR) rates demand urgent development of non-antibiotic strategies.[9,10] Plant-derived therapeutics have been regarded as promising alternatives, with over 60% of recently investigated anti-mastitis compounds originating from botanical sources. Nevertheless, conventional phytochemical extraction methods face critical limitations: (1) compromised bioactivity through isolation of single compounds and (2) suboptimal bioavailability (<15% for most polyphenols).[11,12] The above obstacles seriously hinder their clinical application.

Plant-derived extracellular vesicles (PEVs) are nanovesicles with a particle size of 30–200 nm extracted from various edible vegetables, fruits and medicinal plants, which contain a variety of bioactive components such as proteins, lipids, nucleic acids, *etc.*[13] PEVs offer distinct advantages, including scalability in production[14,15] and enhanced safety due to the absence of animal pathogens[16,17] and have shown great advantages in the treatment of many diseases.[18,19] For example, ginseng-derived PEVs exhibited cardioprotective effects against cisplatin-induced injury through the modulation of the MAPK signaling pathway and improved the efficiency of cisplatin in treating cancer.[20,21] Platycodon grandiflorum-derived PEVs suppressed triple-negative breast cancer by strengthening systemic immunity and modulating the gut microbiota.[22] Momordica-derived PEVs

[a] Jilin Provincial International Cooperation Key Laboratory for Science and Technology Innovation of Special Animal and Plants, Institute of Special Animal and Plant Sciences, Chinese Academy of Agricultural Sciences, Changchun, Jilin, 130112, China. E-mail: pengyinghua@caas.cn, yangmin01@caas.cn
[b] School of Chemistry and Life Science, Changchun University of Technology, Changchun, Jilin, 130012, China

† Electronic supplementary information (ESI) available. See DOI: https://doi.org/10.1039/d5tb00861a

alleviated blood–brain barrier damage in the model and inhibited neuronal apoptosis by promoting the AKT/GSK3β signaling pathway.[23] Thus, harnessing PEVs, particularly those isolated from medicinal plants, represents a promising therapeutic strategy for mastitis treatment.

Taraxacum mongolicum Hand.-Mazz. is a kind of perennial herbaceous plant of the Asteraceae family, widely distributed across the warm temperate regions of the Northern hemisphere on the slopes, grasslands, roadsides, *etc.* As a plant with medicinal and edible homologous, *Taraxacum mongolicum* Hand.-Mazz. has been regarded as a superior medicine for clearing heat and detoxifying, reducing stasis and swelling and treating mastitis since ancient times.[24,25] Contemporary pharmacological investigations have revealed that *Taraxacum mongolicum* Hand.-Mazz. has a diverse many of bioactive compounds, including phenolic acids, polysaccharides, and flavonoids, which exhibit multiple pharmacological properties such as antimicrobial,[26,27] anti-inflammatory,[28] antioxidant,[29] immunomodulatory, anti-tumor, and breast disease. The therapeutic effects of *Taraxacum mongolicum* Hand.-Mazz. extracts on breast diseases have been extensively studied. For instance, *Taraxacum mongolicum* Hand.-Mazz. extracts could effectively alleviate oxidative damage in bovine mammary epithelial cells (BMECs) through activation of the Nrf2 pathway.[30] Additionally, chlorogenic acid derived from Taraxacum officinale had been demonstrated to reduce lipoteichoic acid (LTA)-induced inflammation in BMECs by inhibiting the phosphorylation of proteins within the NF-κB pathway.[31] Nonetheless, the bioavailability of these components is relatively low (2-5%),[32] which hinders its clinical application. In addition, in contrast to synthetic reagents, PEVs possess excellent biocompatibility and exhibit extremely low immunogenicity.[33] Their inherent lipid bilayer structure circumvents the drawbacks associated with synthetic materials, such as accelerated blood clearance and inflammatory responses.[34] Meanwhile, PEVs are rich in bioactive molecules (such as proteins, lipids, nucleic acids), which have similar effects to the original plants and can synergistically enhance the therapeutic effect. Currently, research on TH-EVs is still relatively limited. Studies have demonstrated that TH-EVs effectively reduced indirect hypoxia-induced hypertension by modulating gut microbes.[35] In addition, TH-EVs-laden hydrogels were capable of neutralizing *Staphylococcus aureus* exotoxins, aiding in the treatment of invasive wounds.[36] We assumed that the natural origin and synergistic multicomponent cargo of PEVs from *Taraxacum mongolicum* Hand.-Mazz. may overcome the bioavailability limitations of conventional phytochemicals and address the pressing need for non-antibiotic alternatives in combating mastitis.

In the current study, PEVs derived from *Taraxacum mongolicum* Hand.-Mazz. (TH-EVs) were extracted through ultracentrifugation and sucrose gradient centrifugation. We determined their morphology and particle size characteristics and proteins and nucleic acid distribution. The effects of TH-EVs in LPS-induced murine mammary epithelial cells were investigated. In addition, their efficacy and the mechanisms in LPS-induced mastitis were evaluated *in vivo* (Scheme 1). Our findings provide a novel therapeutic protocol for the treatment of mastitis and contribute to the development and utilization of *Taraxacum mongolicum* Hand.-Mazz. as a medicinal resource.

2. Materials and methods

2.1. Isolation and identification of TH-EVs

The whole *Taraxacum mongolicum* Hand.-Mazz. was thoroughly washed, cut into small pieces, and then processed into juice. The juice was initially centrifuged at 200×*g*, 10 min, followed by centrifugation at 2000×*g*, 20 min, and finally at 10 000×*g*, 30 min to remove fibers and larger particles (Beckman Coulter, USA). The resulting supernatant was centrifuged at 100 000×*g*, 60 min to obtain the pellet. It was resuspended in phosphate-buffered saline (PBS) and passed through a 0.45 μm filter (Millipore, Burlington, MA). The solution was transferred to a gradient sucrose solution (15%, 30%, 45%, and 60%) and ultracentrifuged at 120 000×*g*, 1 h. The interfacial fraction (30%–45% sucrose gradient) was harvested, subjected to PBS dilution, and filtered using a 0.22 μm membrane. This resulting filtrate underwent ultracentrifugation (100 000×*g*, 1 h), with the resultant pellet either freshly reconstituted in PBS or cryopreserved at −80 °C for future use.

The structural profiling of TH-EVs was evaluated through TEM (JEOL, Tokyo, Japan). The size of TH-EVs was measured *via* nanoflow cytometry (NanoFCM, Xiamen, China). Total RNA was isolated using a nucleic acid extraction kit (Tiangen, Beijing, China). The RNA composition of TH-EVs was analyzed using agarose gel electrophoresis. Protein denaturation was achieved through 5× loading buffer system equilibration (10 min, 100 °C boiling point stabilization). The protein samples were electrophoresed on a 12% resolving phase (Epizyme Biomedical Technology, Shanghai, China) and the protein distribution of TH-EVs was identified by Coomassie Brilliant blue staining.

2.2. Cell culture

Mouse mammary epithelial cell lines (HC11) were purchased from Wuhan Pricella Biotechnology Co., Ltd (Wuhan, China). We grew the cells in Roswell Park Memorial Institute 1640 medium (Gibco, USA) supplemented with 10% fetal bovine serum (FBS) (PAN, Germany) and 1% penicillin–streptomycin (Gibco, USA), and maintained at 37 °C under a 5% CO_2 atmosphere.

2.3. Uptake of TH-EVs by HC11 cells

2 μL of TH-EVs and 1 μL of DII (Beyotime Biotechnology, Shanghai, China) were incubated at 37 °C for 30 min, followed by centrifugation at 150 000×*g*, 90 min. Then, centrifuged particles were resuspended in PBS to obtain DII-TH-EVs. Subsequently, HC11 cells were maintained in 12-well plates with a concentration of 3×10^5 cells per well. Upon achieving approximately 50% confluence, DII-TH-EVs were introduced to the cells and incubated for 12 h. After incubation, the cells were washed with PBS, and the nuclei were treated with 50 μL of

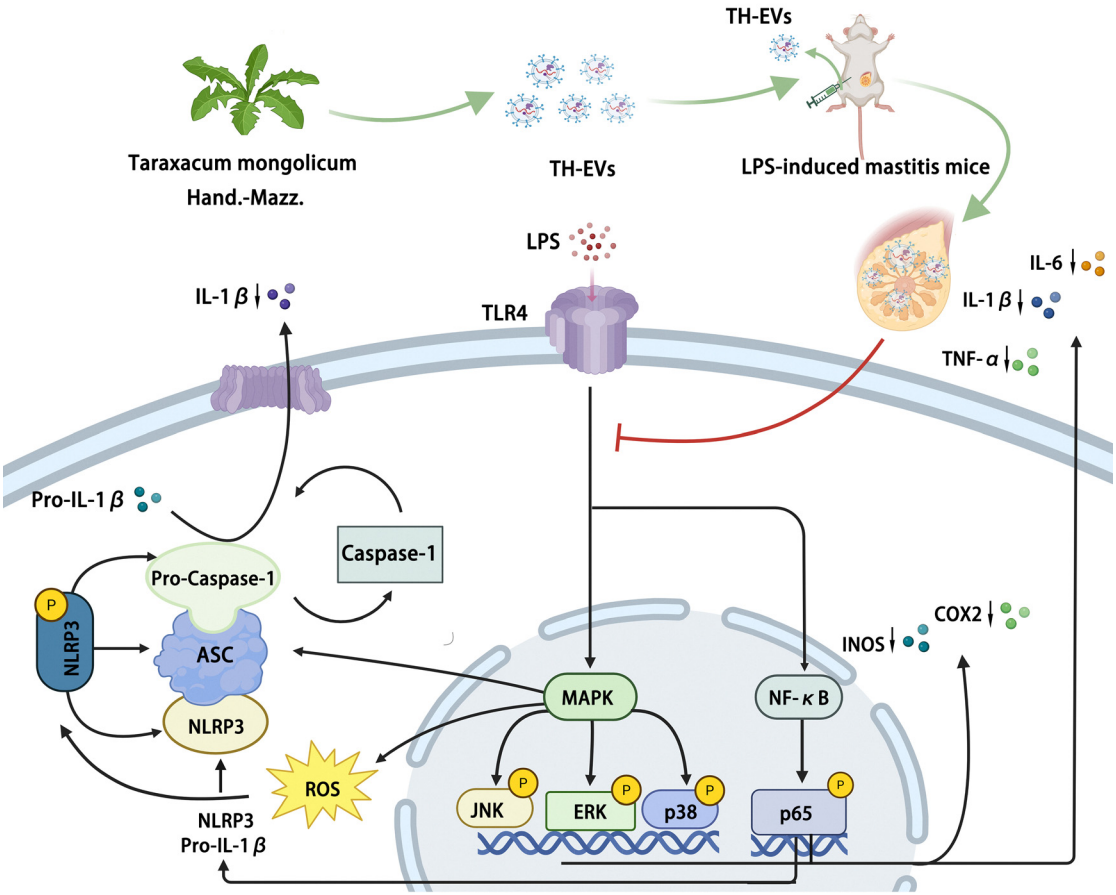

Scheme 1 Protective mechanism of TH-EVs against LPS-induced mastitis in mice.

DAPI for 5 min. Finally, the cells were visualized under a fluorescence microscope (Nikon, Tokyo, Japan).

2.4. Cell viability assays

HC11 cells were seeded in 96-well plates (1×10^5 cells per well). When the seeded cells achieved a confluence of about 60%, the cells were starved for 12 h by changing the medium to 1% FBS. The cells were incubated for 12 h, the medium was discarded, and the cells were treated with TH-EVs at concentrations of 1–40 μg mL^{-1} for 24 h. Subsequently, each well received working fluids (medium: CCK8 = 9 : 1) (KeyGEN Biotechnology, Nanjing, China), after which the cells were cultured at 37 °C for 2 h. The absorbance at 450 nm was measured with a microplate reader to evaluate cell viability. Furthermore, to examine the impact of TH-EVs on the viability of LPS-activated HC11 cells, the cells were categorized into three groups: control group, LPS group (2 μg mL^{-1}), and LPS + TH-EVs (2 μg mL^{-1} + 20 μg mL^{-1}) group. The cell viability in these groups was evaluated using the same method as described above.

2.5. Quantitative real time polymerase chain reaction (qRT-PCR)

6×10^6 HC11 cells per well were cultured with medium with 1% FBS in 6-well plates for 12 h. Then, the cells were divided into control group, LPS group (2 μg mL^{-1}), and LPS + TH-EVs (2 μg mL^{-1} + 20 μg mL^{-1}) group, and cultured in full medium for 24 h. After incubation, the cells were washed three times with PBS, and the total RNA was extracted using the nucleic acid extraction kit (Tiangen, Beijing, China). The mRNA expression levels of TNF-α, IL-1β, IL-6, INOS and COX2, along with NLRP3 inflammasome pathway markers (NLRP3, ASC, and Caspase-1) were assessed using qRT-PCR experiments. The primer sequences of inflammatory genes are indicated in Table S1, ESI.†

2.6. Western blot

Proteins were harvested from HC11 cells under different treatments and from mouse breast tissue using RIPA lysis buffer (KeyGEN BioTECH, Nanjing, China) supplemented with phosphatase inhibitors (Roche, Basel, Switzerland) and protease inhibitors (Roche, Basel, Switzerland), and the protein concentration of each sample was determined using a BCA kit (Thermo Fisher, Waltham, MA, USA). An equal amount of protein was mixed with loading buffer and boiled at 100 °C for 20 min. Next, the protein sample was subjected to electrophoresis on 10% SDS-PAGE (120 V, 90 min) and transferred to a PVDF membrane. Then the membrane was blocked for 40 min at ambient temperature. Then, the membrane was treated

overnight at 4 °C with the primary antibodies, including IL-6, ASC, IL-1β, Caspase-1, p-P65, p-P38, p-JNK, and p-ERK (Abcam, Cambridge, UK). β-actin, GAPDH, INOS, COX2, and NLRP3 (Cell Signaling Technology, Boston, USA). The membranes were then washed 3 times (10 min each) with TBST and incubated for 60 min at room-temperature with secondary antibodies, and then the proteins were visualized and analyzed.

2.7. Animal

SPF-grade ICR pregnant mice (30 ± 2 g) were acquired from Shenyang Changsheng Biotechnology Company (Shenyang, China). These mice were housed at 20–22 °C with 55%–65% humidity and allowed free access to food and water for 7 d. All experimental procedures were conducted in compliance with the guidelines and regulations by the Animal Administration and Ethics Committee of the Institute of Special Animal and Plant Sciences, Chinese Academy of Agricultural Sciences (NO. ISAPSAEC-2023-039TM).

2.8. LPS-induced mouse mastitis model

Lactating mice at 5-7 days postpartum were assigned to the control group, LPS group (2 μg mL^{-1}), LPS + dexamethasone (Dex) (5 mg kg^{-1}) group, LPS + TH-EVs-low group (2 mg kg^{-1}), and LPS + TH-EVs-high group (4 mg kg^{-1}). Dex, a commonly used steroid anti-inflammatory drug, was selected as the positive drug. Initially, the corresponding drugs were intraperitoneally injected into the mice of different groups (the control group and LPS group were injected with physiological saline). After 1 h, the mice were anesthetized, and LPS was injected into their mammary glands *via* the milk ducts. After 12 h, the corresponding drug was injected to the mice again. Then the mice were sacrificed, serum and the fourth pair of breast tissue were taken for testing.

2.9. ELISA

The concentrations of inflammatory cytokine (TNF-α, IL-1β, and IL-6) levels of the mouse serum after TH-EV treatment were detected using the ELISA kit (Shanghai Enzyme linked Biotechnology Co., Ltd, Shanghai, China) according to the manufacturer's directions. Optical density measurements at 450 nm wavelength were acquired through spectrophotometric analysis, with TNF-α, IL-1β, and IL-6 derived from standard curve, expressed in pg mL^{-1}.

2.10. Hematoxylin–eosin (H&E) staining

The collected mammary tissues were embedded in paraffin. Subsequently, the paraffin-embedded samples were sliced into 4-μm-thick sections. They were then stained with H&E dyes. Finally, the slices were observed for histopathological changes under a microscope.

2.11. Immunohistochemical experiments

To explore the expression of TNF-α, IL-6, myeloperoxidase (MPO), and cluster of differentiation 3 (CD3) in breast tissue through immunohistochemical experiments, paraffin slices endogenous enzymatic activity suppression was achieved through immersion in 3% H_2O_2. We treated the sections with TNF-α (Boster, Wuhan, China), IL-6 (Servicebio, Wuhan, China), MPO (Abcam, Cambridge, UK), and CD3 (Abcam, Cambridge, UK) antibodies at 4 °C overnight, followed by incubation with the corresponding secondary antibodies (SeraCare, Massachusetts, USA) for 1 h at room temperature. Then, the DAB chromogenic agent was used for colorimetric development, followed by counterstaining with hematoxylin. Finally, all tissue sections were visualized under a microscope.

2.12. Reactive oxygen species (ROS) staining

Frozen breast tissue slices were reheated and incubated with DHE (Beyotime Biotechnology, Shanghai, China) in the dark at 37 °C for 40 min. After washing the slices with PBS, DAPI solution was added dropwise and the slices were stained for 10 min in the dark at room temperature. Then the stained slices were observed under a fluorescence microscope.

2.13. Data analysis

The results were shown as mean ± standard deviation (SD) and analysis was performed using the Tukey test by Origin 2024 software. Statistical significance was indicated as follows: Compared with the control group, $^{\#}p < 0.05$, $^{\#\#}p < 0.01$, $^{\#\#\#}p < 0.001$; compared with the LPS group, $^{*}p < 0.05$, $^{**}p < 0.01$, $^{***}p < 0.001$.

3. Results

3.1. Identification, characterization and biological activity of TH-EVs

TH-EVs were extracted from fresh *Taraxacum mongolicum* Hand.-Mazz. using ultracentrifugation and sucrose density gradient centrifugation (Fig. 1A). TEM results showed that TH-EVs exhibited cup-shaped vesicles with a bilayer membrane structure (Fig. 1B). The mean size of TH-EVs was measured at 63 nm using nanoflow cytometry (Fig. 1C). SDS-PAGE analysis indicated that the distribution of the proteins in TH-EVs ranged from 25 to 70 kDa (Fig. 1D). RNA extracted from TH-EVs was primarily 250 bp (Fig. 1E). These results demonstrated the successful isolation of TH-EVs. To investigate the uptake of TH-EVs by HC11 cells (mouse mammary epithelial cells), TH-EVs were tagged with the fluorescent dye DII (DII-TH-EVs) and observed using fluorescence microscopy. The results showed that the DII-TH-EVs were abundantly enriched around the nucleus (Fig. 1F), demonstrating that TH-EVs could smoothly enter the cell membrane and be internalized by HC11 cells. In order to detect the toxicity of TH-EVs on HC11 cells, TH-EVs were applied to these cells at graded concentrations ranging from 1 to 40 μg mL^{-1} and the cell viability was measured using the CCK8. These data revealed that TH-EVs did not exhibit toxicity toward HC11 cells at concentrations of 1–20 μg mL^{-1}. However, at the concentration of 40 μg mL^{-1}, the cell viability decreased to 88.6% (Fig. 1G). To further investigate the effect of TH-EVs on the viability of LPS-induced HC11 cells under inflammatory conditions, we conducted the CCK8 experiment.

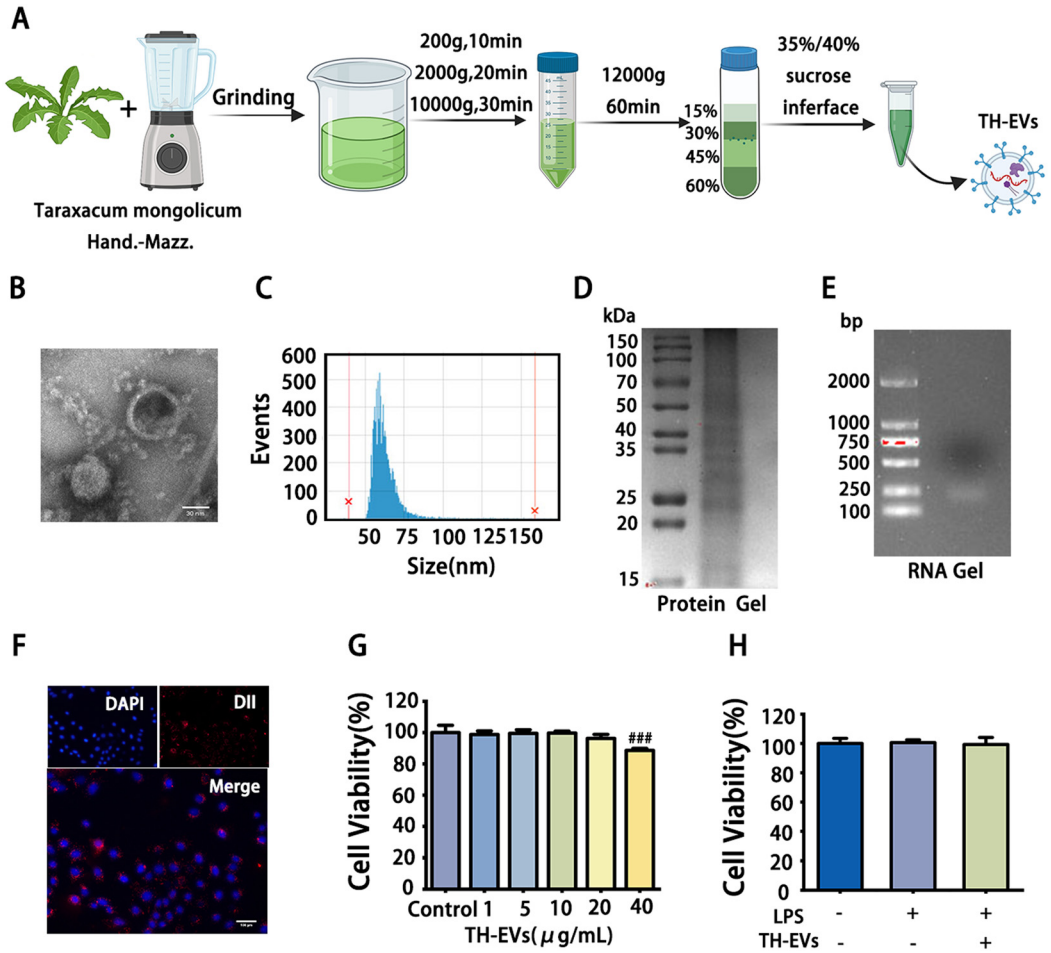

Fig. 1 Identification, characterization and biological activity studies of TH-EVs. (A) Schematic diagram of TH-EVs extraction. (B) TEM was used to observe TH-EVs, scale bar: 30 nm. (C) The dimensions of the TH-EVs. (D) SDS-PAGE gel electrophoresis of TH-EVs proteins. (E) Agarose gel electrophoresis of TH-EVs RNAs. (F) Representative fluorescence image of HC11 cells uptake of DII-labeled, scale bar: 100 μm. (G) Effect of TH-EVs (0–40 μg mL^{-1}) on HC11 cell viability. (H) Effect of TH-EVs on LPS-induced HC11 cell viability (n = 3).

The data showed that treatment with 20 μg mL^{-1} TH-EVs did not affect the viability of HC11 cells under the inflammatory state induced by LPS (Fig. 1H). Based on these results, the concentration of 20 μg mL^{-1} TH-EVs was selected for subsequent experiments to explore their effects on the inflammatory response of LPS-induced HC11 cells.

3.2. TH-EVs alleviate LPS-induced inflammation in HC11 cells

In order to simulate breast inflammation *in vitro*, the HC11 cells were treated with LPS. For testing the effect of TH-EVs on HC11 cell inflammation, the qRT-PCR tests were performed to analyze the gene expression profiles of TNF-α, IL-1β, IL-6, INOS and COX2 (Fig. 2A–E). The data clarified that LPS stimulation conspicuously raised the gene expression levels of TNF-α, IL-6, IL-1β, INOS, and COX2 in HC11 cells. However, exposure to TH-EVs (20 μg mL^{-1}) decreased the gene expression levels of these factors. Moreover, the protein expressions of IL-1β, IL-6, and COX2 in HC11 cells were detected by western blot. LPS induction led to a significant increase in the expression of these proteins (Fig. 2F–I). Nevertheless, after treatment with TH-EVs (20 μg mL^{-1}), there was a marked reduction in the levels of IL-1β, IL-6, and COX2. These results collectively demonstrated that TH-EVs could alleviate the inflammatory response in LPS-induced HC11 cells.

3.3. TH-EVs ameliorate LPS-induced HC11 cell inflammation through the inhibition of NLRP3 inflammasomes, NF-κB and MAPK pathways

It is well known that the occurrence of inflammation is influenced by a variety of pathways, among which the activation of NLRP3 inflammasome, NF-κB and MAPK pathways are essential for inflammatory response regulation. In order to explore the mechanism of TH-EVs on LPS-induced HC11 cells, qRT-PCR was utilized to detect the expression profiles of NLRP3 inflammasome signaling pathway marker genes in LPS-induced HC11 cells. As indicated in Fig. 3A–C, TH-EVs treatment appreciably inhibited the expressions of NLRP3, ASC, and Caspase-1 in LPS-induced HC11 cells. Furthermore, the expressions of the NLRP3 signaling pathway markers NLRP3, ASC, and Caspase-1, the NF-κB signaling pathway marker protein

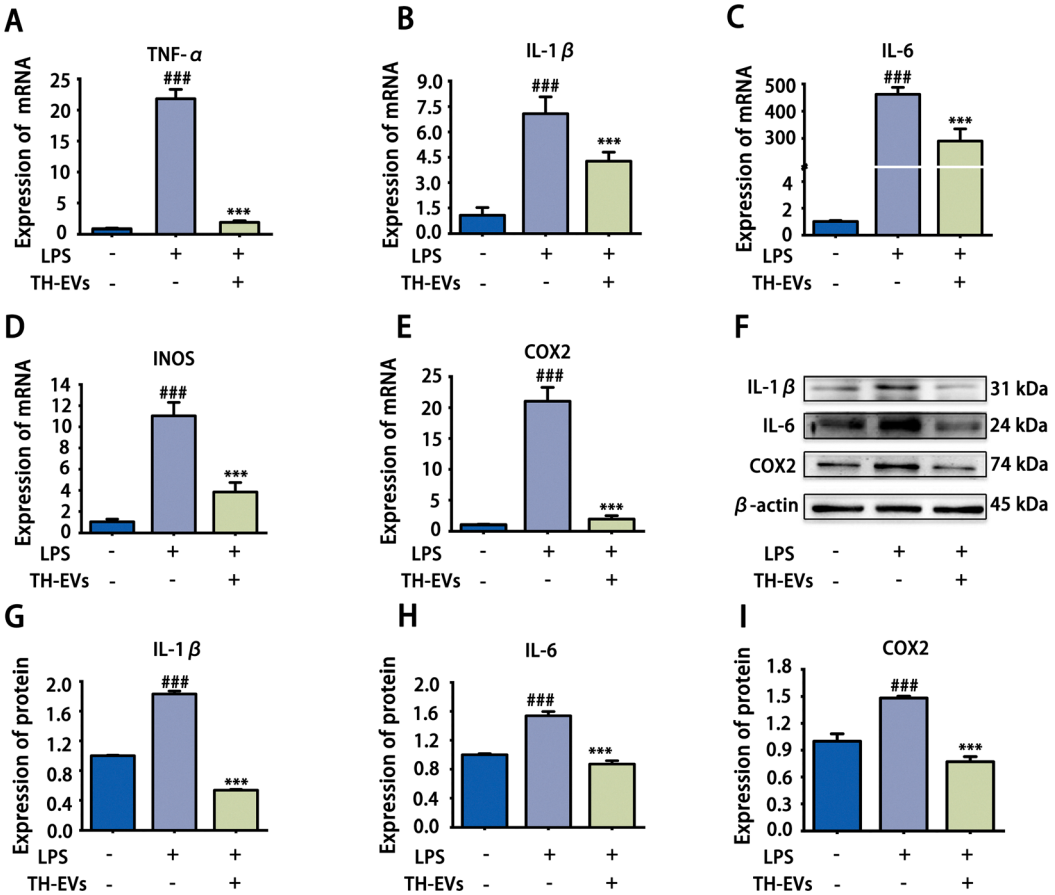

Fig. 2 TH-EVs attenuate inflammation in HC11 cells following LPS exposure. qRT-PCR experiments were used to detect the expression of TNF-α (A), IL-1β (B), IL-6 (C), INOS (D) and COX2 (E) in HC11 cells in control group, LPS (2 μg mL^{-1}) and LPS + TH-EVs (2 μg mL^{-1} + 20 μg mL^{-1}) groups. Western blot analysis (F) and quantification results of IL-1β (G), IL-6 (H) and COX2 (I) expressions in HC11 cells in control, LPS (2 μg mL^{-1}) and LPS + TH-EVs (2 μg mL^{-1} +20 μg mL^{-1}) groups (n = 3).

p-P65, and the MAPK signaling pathway marker protein in HC11 cells were analyzed. The results showed that LPS administration greatly enhanced the levels of ASC, NLRP3, Caspase-1, p-P65, p-JNK, p-ERK, and p-P38 protein. However, in contrast to the LPS group, the expression of these proteins in TH-EVs groups were considerably reduced (Fig. 3D–L). These findings strongly suggested that TH-EVs could attenuate inflammation in HC11 cells by targeting the NLRP3 inflammasome, NF-κB, and MAPK pathways.

3.4. TH-EVs attenuate LPS-induced mastitis in mice

To investigate the effects of TH-EVs on mastitis *in vivo*, we established a mouse model of mastitis. Breast tissues were collected 24 h after LPS induction and TH-EVs treatment (Fig. 4A). Observing the mammary gland tissue of mice in different groups, we found that TH-EVs treatment remarkably improved the inflammatory response of redness, swelling, and congestion in the mammary gland tissue induced by LPS (Fig. 4B). Moreover, H&E staining was carried out to explore structural differences in mammary tissue across different treatment groups. The results implied that LPS led to the disappearance of the acinar cavity structure in mammary tissue, with a large number of inflammatory cells and exudates observed in the acinar cavity. In contrast, treatment with TH-EVs distinctly mitigated the histopathological changes in mouse mammary glands induced by LPS (Fig. 4C). In order to further confirm the inflammatory changes in mice, an immunohistochemistry experiment was carried out to evaluate the protein expressions of inflammatory cytokine. These findings suggested that LPS stimulation resulted in a significant increase in the expression of TNF-α, and IL-6, while TH-EVs treatment remarkably inhibited this effect (Fig. 4D). To further determine the variations in the inflammatory response in mice, ELISA was used to detect the levels of inflammatory cytokines in mouse serum after different treatments. As shown in (Fig. 5A–C), these inflammatory cytokine concentrations in the LPS group were substantially higher than in the control group. However, they were considerably downgraded in mastitis mice after TH-EVs treatment. These results were similar to those from immunohistochemistry experiments, further indicating that TH-EVs could reduce the inflammatory response in mastitis mice. MPO, as a peroxidase enzyme, is a key marker of neutrophil activation. Given that neutrophils play a central role in inflammatory response, MPO levels can sensitively reflect the

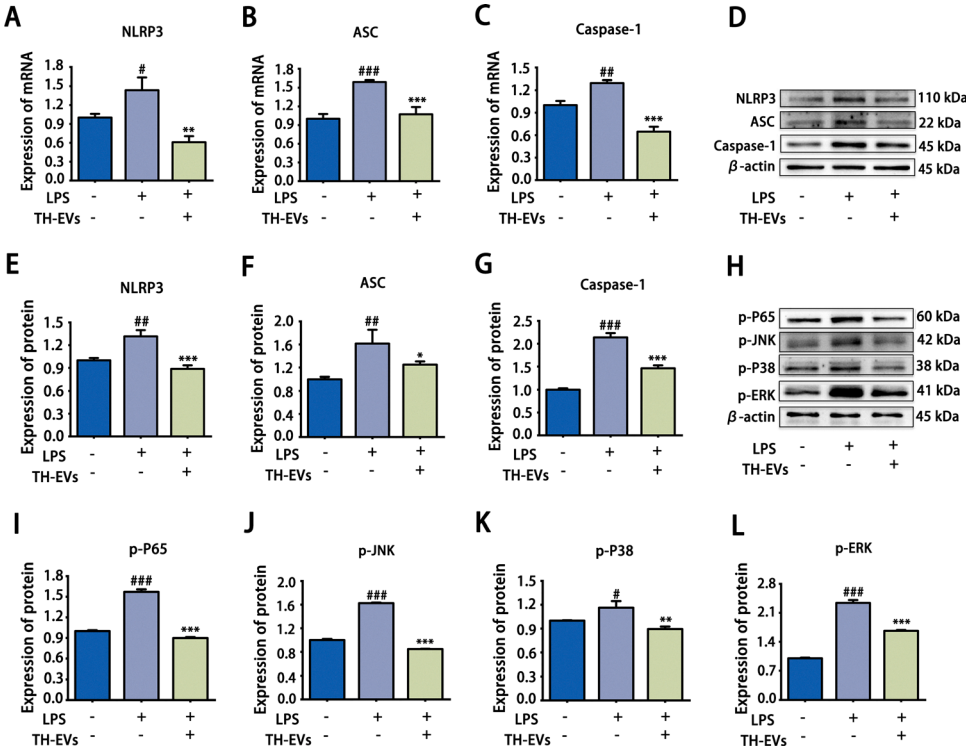

Fig. 3 TH-EVs ameliorate LPS-induced inflammation in HC11 cells by targeting the activation of the NLRP3 inflammasomes, NF-κB, and MAPK pathways. qRT-PCR was employed to detect the levels of NLRP3 inflammasome pathway key marker genes NLRP3 (A), ASC (B) and Caspase-1 (C) in different treatment groups. Western blot analysis (D) and quantification results of NLRP3 inflammasome signaling pathway marker proteins NLRP3 (E), ASC (F) and Caspase-1 (G) in different treatment groups. Western blot evaluation (H) and quantification of NF-κB signaling marker proteins p-P65 (I) and MAPK signaling pathway markers p-JNK (J), p-P38 (K), and p-ERK (L) in HC11 cells with different treatment groups (n = 3).

presence and degree of inflammation.[37] Therefore, we additionally measured the MPO levels in breast tissue through immunohistochemistry experiments (Fig. 5D). The findings indicated that MPO was considerably higher in the LPS group than in the control group. The control group, whereas TH-EVs treatment markedly reduced MPO levels. ROS, which caused oxidative stress, also played a major role in the inflammatory process.[38,39] Therefore, we further measured the production of ROS in breast tissues through fluorescence staining. The data presented that ROS fluorescence in breast tissues was notably boosted after LPS stimulation, and could be inhibited by TH-EVs treatment (Fig. 5E). CD3 is a pivotal marker of T lymphocytes, prominently displayed on their membrane surface. It exerts significant influence on inflammation, immune diseases, and cancer.[40] Herein, CD3 in breast tissues was assessed by immunohistochemistry. (Fig. 5F) indicated that the expression of CD3 increased after LPS stimulation and decreased after TH-EVs treatment. The above results underscore that TH-EVs could attenuate oxidative stress and tissue damage in mastitis mice, thereby alleviating the inflammatory response.

3.5. TH-EVs ameliorate LPS-induced mastitis in mice by preventing NLRP3 inflammasome, NF-κB, and MAPK pathways

The NLRP3 inflammasome, NF-κB and MAPK signaling pathway play crucial roles in regulating the inflammatory response. To further explore the underlying anti-inflammatory mechanisms of TH-EVs, we detected the expression of NLRP3 inflammasome signaling pathway markers ASC, Caspase-1 (Fig. 6A–C) and the NF-κB signaling marker p-P65 (Fig. 6D and E), and MAPK signaling pathway markers p-JNK, and p-ERK (Fig. 6F–H) in breast tissues of mice after various treatments by western blot experiments. The data revealed that LPS treatment hugely upgraded the protein expressions of ASC, Caspase-1, p-P65, p-JNK, and p-ERK. By contrast, TH-EVs administration greatly lowered the expression of these proteins. The findings implied that TH-EVs could attenuate LPS-induced mastitis in mice by targeting the activation of NLRP3 inflammasome, NF-κB and MAPK pathways.

4. Discussion

Mastitis is a common disease that poses significant threats to human health.[41] As a well-known medicinal and edible homologous plant, *Taraxacum mongolicum* Hand.-Mazz. is regarded as a superior medicine for heat-clearing and detoxifying properties, diminishing swelling, and resolving stasis, especially in the treatment of breast diseases.[42] *Taraxacum officinale* sterol, the principal bioactive component of *Taraxacum mongolicum* Hand.-Mazz., exhibits anti-inflammatory effects by reducing cellular oxidative stress and modulating the production of pro-inflammatory cytokines and mediators.[43,44] However, it comprises diverse compounds, including carotene, stigmasterol, and β-sitosterol, with a complicated composition that

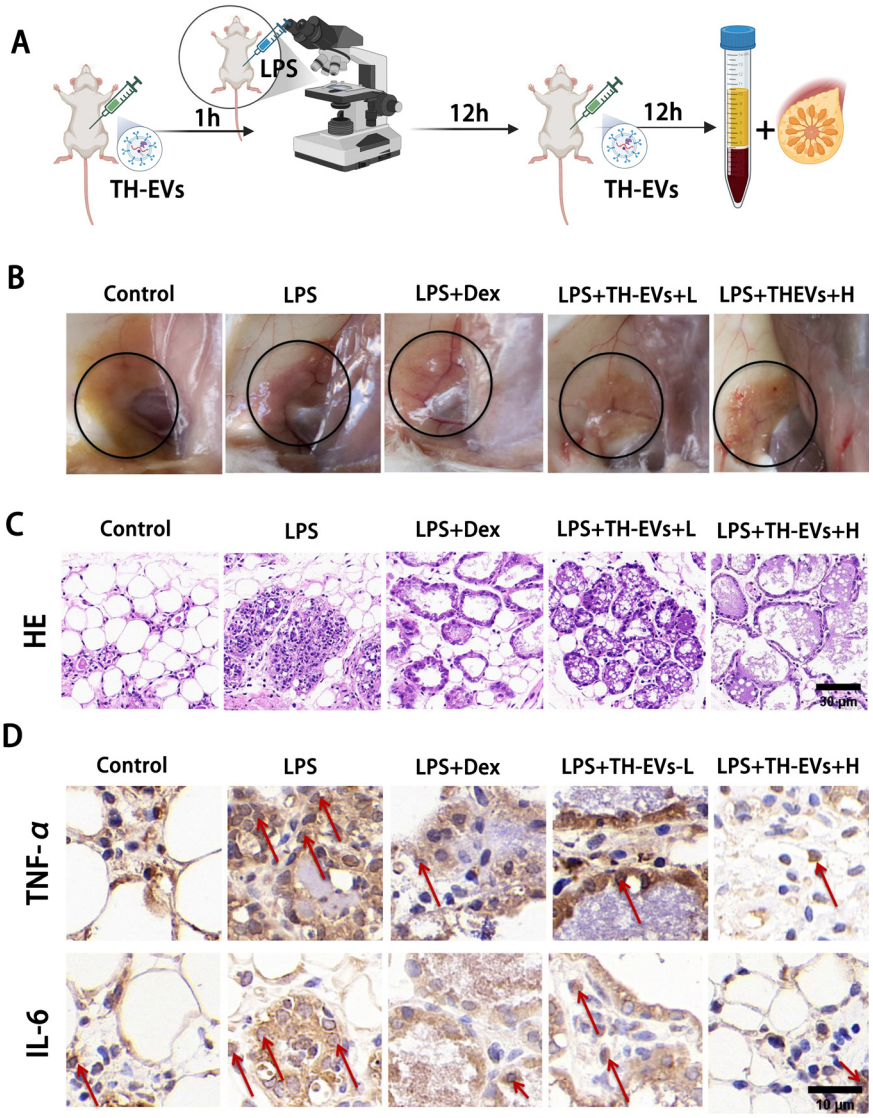

Fig. 4 TH-EVs attenuate mastitis in mice *in vivo*. (A) Schematic diagram of animal experiments. (B) Breast tissues across distinct treatment groups. (C) H&E staining images depicting mammary gland tissue of mice across different regimens, scale bar: 30 μm. (D) Immunohistochemical staining images of TNF-α and IL-6 in mammary gland tissue from different treatment groups, scale bar: 10 μm (n = 6).

poses challenges for pharmacological research. Additionally, the low utilization rate of plant sterols, at merely 2–5%, impedes their clinical application.[32] In contrast, the nanoscale (63 nm) of the TH-EVs we extracted facilitates cell membrane penetration (Fig. 1B). Their bilayer lipid membrane structure not only provides superior protection for the contents but also enhances fusion with target cell membranes,[45] thereby overcoming the restrictions of limited cellular uptake and bioavailability of *Taraxacum mongolicum* Hand.-Mazz. sterol. Specific proteins on the membrane of TH-EVs are capable of recognizing specific protein receptors, thereby achieving targeted delivery. This mechanism enables the direct release of contents into the cytoplasm, avoiding lysosomal degradation.[46] Compared to synthetic liposomes, TH-EVs exhibit superior stability, stronger delivery capacity, and higher utilization efficiency.[47] Owing to their natural plant origin, TH-EVs possess lower cytotoxicity and higher biocompatibility compared to synthetic materials. As demonstrated by the CCK-8 assay in this study (Fig. 1G–H), TH-EVs maintain low toxicity on HC11 cells even at a high level of 40 μg mL^{-1}. Furthermore, unlike single active ingredients, TH-EVs contain diverse bioactive substances, including proteins and RNAs (Fig. 1D and E), which exert synergistic effects, resulting in a more comprehensive therapeutic outcome. *In vitro* studies demonstrated that TH-EVs, exhibited remarkable anti-inflammatory effects by inhibiting the production of inflammatory factors (Fig. 2).

In a murine mastitis model, TH-EVs administered *via* intraperitoneal injection significantly alleviated LPS-induced mastitis with reduced inflammatory cytokine levels in both serum and mammary tissue (Fig. 4D and 5A–C). MPO and ROS levels were significantly reduced, indicating that TH-EVs diminished inflammatory cell infiltration and alleviated oxidative stress.

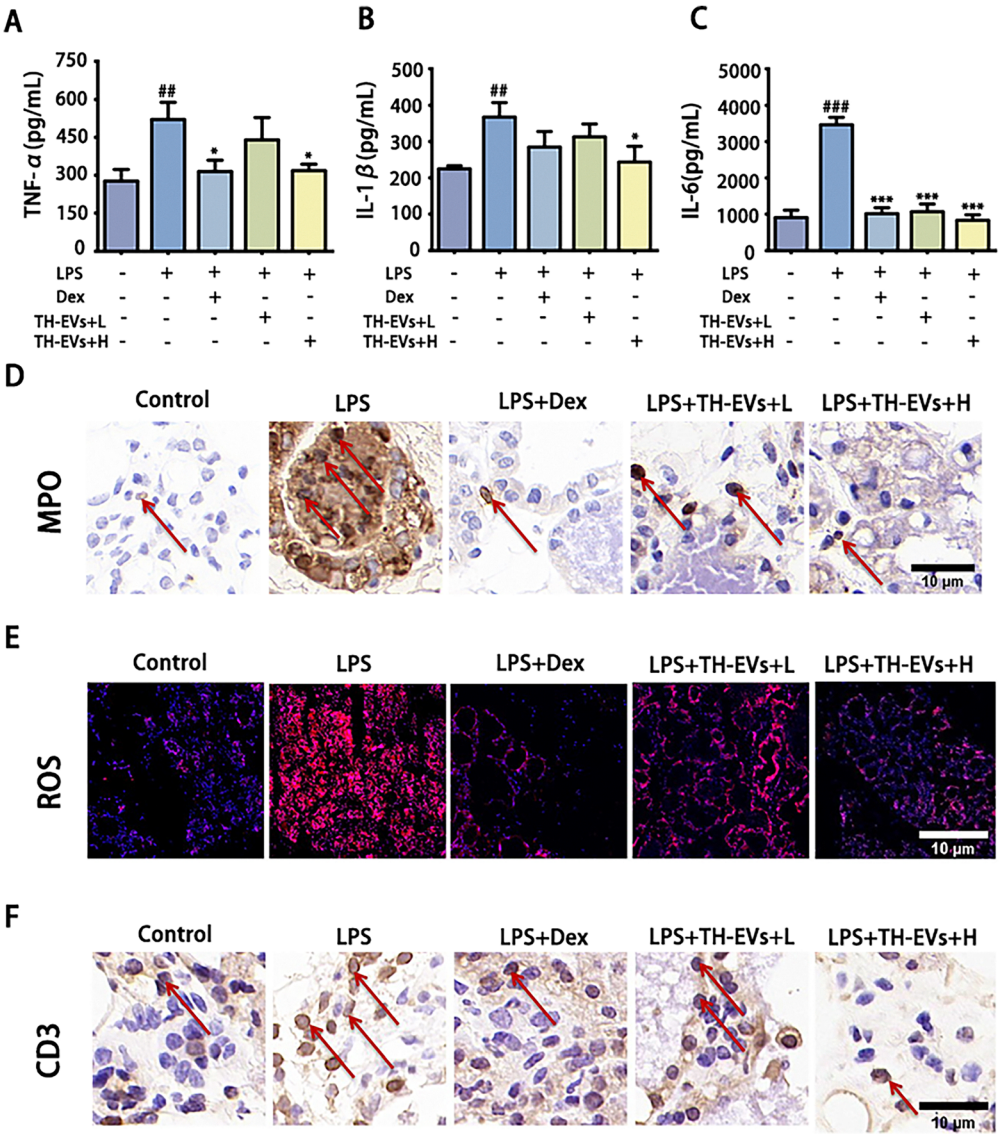

Fig. 5 TH-EVs attenuate LPS-induced mastitis in mice *in vivo*. The concentrations of TNF-α (A), IL-1β (B), and IL-6 (C) were detected in the serum of mice from different treatment groups using ELISA. (D) Immunohistochemistry staining was used to detect the expression of MPO in breast tissues of mice in different treatment groups, scale bar: 10 μm. (E) Fluorescence images of ROS in breast tissues of mice across various treatment groups, scale bar: 10 μm. (F) Immunohistochemistry staining was performed to evaluate the expression of CD3 in different treatment groups, scale bar: 10 μm (n = 6).

Moreover, TH-EVs treatment markedly decreased CD3 expression in breast tissue, thereby inhibiting excessive immune responses through the regulation of the activation balance of T lymphocytes. In conclusion, TH-EVs ameliorated breast tissue damage by alleviating oxidative stress, reducing inflammatory cell infiltration, and suppressing T cell activation.

Confirming the anti-inflammatory properties of TH-EVs in LPS-induced mastitis, we investigated the underlying mechanisms. The inflammasome, NF-κB and MAPK pathways are crucial regulators of the inflammatory response. Upon LPS stimulation, toll like receptor 4 (TLR4) activates NF-κB and MAPK *via* the MyD88-dependent signaling pathway, thereby inducing cytokine release.[48,49] NF-κB, acts as the master switch, which synergistically activates inflammatory response with MAPK. Upon activation, NF-κB triggers the production of NLRP3 and pro-IL-1β, which are essential for activating the NLRP3 pathway. Meanwhile, MAPK pathway activation promotes NLRP3 pathway activation by regulating ROS production and ASC oligomerization. After the NF-κB and MAPK pathways are activated, pro-inflammatory factors and the NLRP3 inflammasome are upregulated, leading to the release of inflammatory mediators. The synergistic interaction between MAPK and NF-κB further exacerbates the inflammatory response.[50,51] In this study, TH-EVs not only directly inhibited the inflammatory factors produced by the NF-κB and MAPK pathways themselves but also indirectly deprived the essential substrates and signals for NLRP3 inflammasome pathway activation (Fig. 6). Compared with single-pathway drugs, TH-EVs exhibited stronger anti-inflammatory

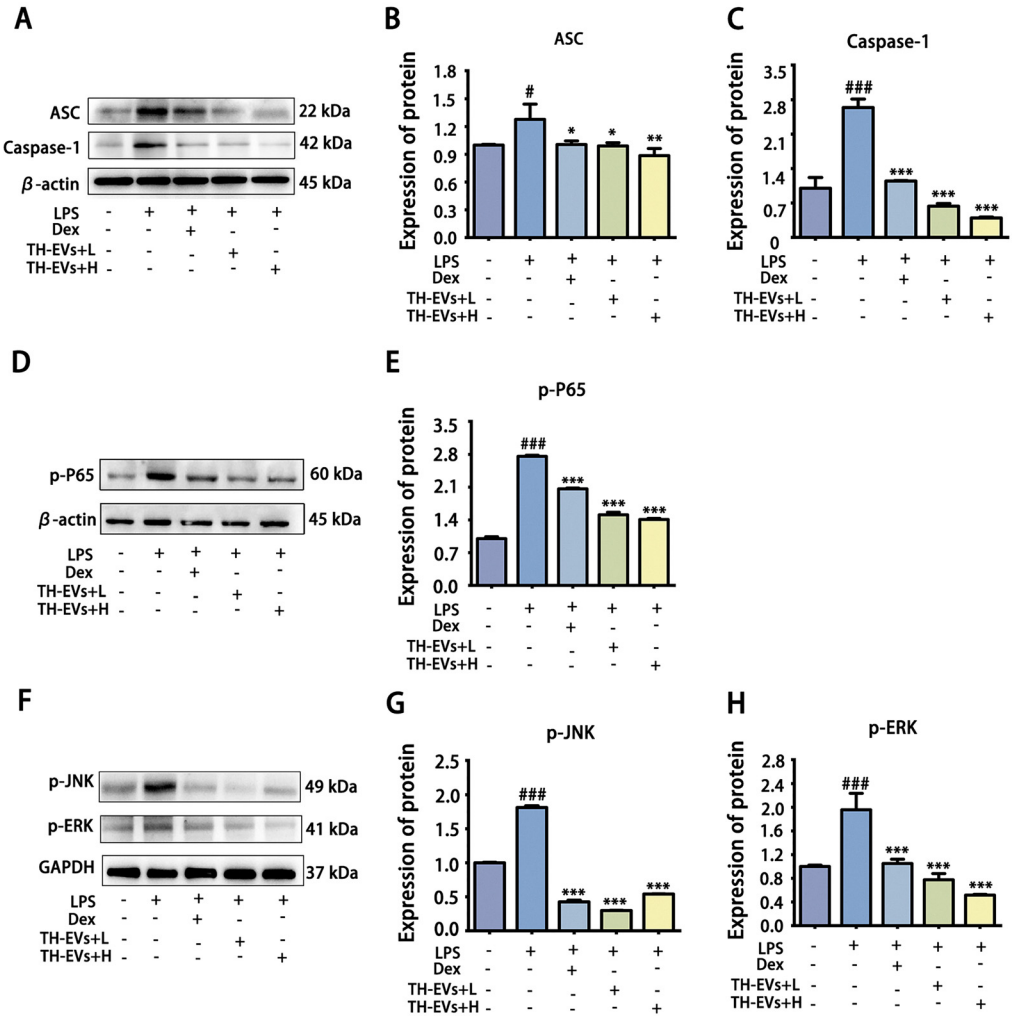

Fig. 6 TH-EVs ameliorate LPS-induced mastitis in mice by inhibiting the NLRP3 inflammasome, NF-κB, and MAPK signaling pathways. Western blot (A) and quantification results of the expression of NLRP3 inflammasome pathway markers ASC (B) and Caspase-1 (C) in breast tissue among mice in distinct treatment groups. Western blot (D) and associated quantification results of the expression of NF-κB signaling marker p-P65 (E) in the mammary gland tissues of mice from various treatment protocols. Western blot (F) and quantification results of the expression of MAPK signaling markers p-JNK (G) and p-ERK (H) in breast tissues of mice in different treatment groups (n = 6).

effects through multi-target synergy. Additionally, their natural origin endowed them with higher safety and reduced side effects, offering a novel therapeutic strategy for mastitis treatment.

5. Conclusions

In summary, TH-EVs were successfully isolated from *Taraxacum mongolicum* Hand.-Mazz. by ultracentrifugation and sucrose gradient centrifugation, and their physicochemical properties were characterized. We investigated the therapeutic potentials and mechanisms of TH-EVs in treating mastitis in both *in vitro* and *in vivo* models. The data demonstrated that TH-EVs significantly reduced the levels of inflammatory cytokines TNF-α, IL-1β, and IL-6 and decreased the expression of MPO, ROS, and CD3 in mammary tissues by blocking the triggering of the NLRP3 inflammasome, NF-κB, and MAPK pathways, thereby alleviating mastitis damage in mice. Our work highlights TH-EVs as a natural and potent nanotherapeutic agent for mastitis.

Author contributions

Yuan Sun: investigation, methodology, validation, and writing – original draft. Ying Liu: investigation and methodology. Jinxian Li: methodology. Shan Huang: methodology. Yiyang Du: methodology. Danyang Chen: writing – review & editing. Min Yang: methodology, supervision, and writing – review & editing. Yinghua Peng: funding acquisition, resources, supervision, and writing – review & editing.

Conflicts of interest

The authors have no conflicts to declare.

Data availability

The data supporting the findings of this study are available within the article and its ESI.† Requests for access to additional data should be directed to the corresponding author.

Acknowledgements

This work was supported by the Science and Technology Innovation Program of the Chinese Academy of Agricultural Sciences (No. CAAS-ASTIP-2021-ISAPS). BioRender.com served as the platform for creating the scheme diagram (Agreement number: TL284E9YPB).

References

1 G. A. Contreras and J. M. Rodriguez, *J. Mammary Gland Biol. Neoplasia*, 2011, **16**, 339–356.
2 M. Endo, T. Konishi, H. Yamana, T. Jo, T. Ishikawa and H. Yasunaga, *J. Obstet. Gynaecol. Res.*, 2024, **50**, 113–119.
3 R. Omranipour and M. Vasigh, *Adv. Exp. Med. Biol.*, 2020, **1252**, 53–61.
4 J. P. Spencer, *Am. Fam. Physician*, 2008, **78**, 727–731.
5 D. Shao, W. Shen, Y. Miao, Z. Gao, M. Pan, Q. Wei, Z. Yan, X. Zhao and B. Ma, *J. Anim. Sci. Biotechnol.*, 2023, **14**, 61.
6 M. Guo, N. Zhang, D. Li, D. Liang, Z. Liu, F. Li, Y. Fu, Y. Cao, X. Deng and Z. Yang, *Int. Immunopharmacol.*, 2013, **16**, 125–130.
7 E. K. Ganda, R. S. Bisinotto, D. H. Decter and R. C. Bicalho, *PLoS One*, 2016, **11**, e0155314.
8 A. C. Kauf, B. T. Vinyard and D. D. Bannerman, *Res. Vet. Sci.*, 2007, **82**, 39–46.
9 J. Tong, X. Hou, D. Cui, W. Chen, H. Yao, B. Xiong, L. Cai, H. Zhang and L. Jiang, *Carbohydr. Polym.*, 2022, **278**, 118910.
10 M. Chu, M. B. Zhang, Y. C. Liu, J. R. Kang, Z. Y. Chu, K. L. Yin, L. Y. Ding, R. Ding, R. X. Xiao, Y. N. Yin, X. Y. Liu and Y. D. Wang, *Sci. Rep.*, 2016, **6**, 24748.
11 L. Zhao, L. Jin and B. Yang, *J. Cell. Mol. Med.*, 2023, **27**, 3443–3450.
12 Y. Xie, X. Li, D. Xu, D. He, J. Wang, J. Bi, J. Liu and S. Fu, *J. Agric. Food Chem.*, 2024, **72**, 21503–21519.
13 Y. Min, P. Li, Y. Shuiyue, C. Ze, G. Jia, L. Ying, C. Shuzhuo and P. Yinghua, *Chem. Eng. J.*, 2024, **479**, 147421.
14 J. Kim, S. Li, S. Zhang and J. Wang, *Asian J. Pharm. Sci.*, 2022, **17**, 53–69.
15 N. Mu, J. Li, L. Zeng, J. You, R. Li, A. Qin, X. Liu, F. Yan and Z. Zhou, *Int. J. Nanomed.*, 2023, **18**, 4987–5009.
16 H. A. Dad, T. W. Gu, A. Q. Zhu, L. Q. Huang and L. H. Peng, *Mol. Ther.*, 2021, **29**, 13–31.
17 M. Cao, N. Diao, X. Cai, X. Chen, Y. Xiao, C. Guo, D. Chen and X. Zhang, *Mater. Horiz.*, 2023, **10**, 3879–3894.
18 J. Kim, S. Li, S. Zhang and J. Wang, *Asian J. Pharm. Sci.*, 2022, **17**, 53–69.
19 M. Cao, N. Diao, X. Cai, X. Chen, Y. Xiao, C. Guo, D. Chen and X. Zhang, *Mater. Horiz.*, 2023, **10**, 3879–3894.
20 S. Yang, J. Guo, D. Chen, Z. Sun, L. Pu, G. Sun, M. Yang and Y. Peng, *ACS Appl. Bio Mater.*, 2025, **8**, 814–824.
21 S. Yang, J. Guo, S. Huang, Z. Sun, M. Yang and Y. Peng, *Biochem. Biophys. Res. Commun.*, 2025, **758**, 151658.
22 M. Yang, J. Guo, J. Li, S. Wang, Y. Sun, Y. Liu and Y. Peng, *J. Nanobiotechnol.*, 2025, **23**, 92.
23 H. Cai, L. Y. Huang, R. Hong, J. X. Song, X. J. Guo, W. Zhou, Z. L. Hu, W. Wang, Y. L. Wang, J. G. Shen and S. H. Qi, *Front. Pharmacol.*, 2022, **13**, 908830.
24 M. Fan, X. Zhang, H. Song and Y. Zhang, *Molecules*, 2023, **28**, 5022.
25 Q. Yan, Q. Xing, Z. Liu, Y. Zou, X. Liu and H. Xia, *Biomed. Pharmacother.*, 2024, **179**, 117334.
26 A. Zhou, S. Zhang, C. Yang, N. Liao and Y. Zhang, *Adv. Clin. Exp. Med.*, 2022, **31**, 529–538.
27 H. Dong, J. Qiao, S. Hou, H. Ran, W. Sun, B. Lin, Y. Han, C. Yu and Y. Li, *Chem. Biodivers.*, 2024, **21**, e202400140.
28 S. Zhou, Z. Wang, Y. Hao, P. An, J. Luo and Y. Luo, *Nutrients*, 2023, **15**, 4120.
29 L. Kang, M. S. Miao, Y. G. Song, X. Y. Fang, J. Zhang, Y. N. Zhang and J. X. Miao, *J. Ethnopharmacol.*, 2021, **281**, 114514.
30 Y. Sun, Y. Wu, Z. Wang, J. Chen, Y. Yang and G. Dong, *Toxins*, 2020, **12**, 496.
31 P. Xu, X. Xu, H. Fotina and T. Fotina, *PLoS One*, 2023, **18**, e0282343.
32 A. Berger, P. J. H. Jones and S. S. Abumweis, *Lipids Health Dis.*, 2004, **3**, 5.
33 J. Bader, F. Brigger and J. Leroux, *Adv. Drug Delivery Rev.*, 2024, **215**, 115461.
34 M. Yanez-Mo, P. R. Siljander, Z. Andreu, A. B. Zavec, F. E. Borras, E. I. Buzas, K. Buzas, E. Casal, F. Cappello, J. Carvalho, E. Colas, A. Cordeiro-da Silva, S. Fais, J. M. Falcon-Perez, I. M. Ghobrial, B. Giebel, M. Gimona, M. Graner, I. Gursel, M. Gursel, N. H. H. Heegaard, A. Hendrix, P. Kierulf, K. Kokubun, M. Kosanovic, V. Kralj-Iglic, E. Kramer-Albers, S. Laitinen, C. Lasser, T. Lener, E. Ligeti, A. Line, G. Lipps, A. Llorente, J. Lotvall, M. Mancek-Keber, A. Marcilla, M. Mittelbrunn, I. Nazarenko, E. N. M. Nolte-'T Hoen, T. A. Nyman, L. O'Driscoll, M. Olivan, C. Oliveira, E. Pallinger, H. A. Del Portillo, J. Reventos, M. Rigau, E. Rohde, M. Sammar, F. Sanchez-Madrid, N. Santarem, K. Schallmoser, M. S. Ostenfeld, W. Stoorvogel, R. Stukelj, S. G. Van der Grein, M. H. Vasconcelos, M. H. M. Wauben and O. De Wever, *J. Extracell. Vesicles*, 2015, **4**, 27066.
35 X. Zhang, Z. Pan, Y. Wang, P. Liu and K. Hu, *Biomed. Pharmacother.*, 2023, **161**, 114572.
36 S. Tan, Z. Liu, M. Cong, X. Zhong, Y. Mao, M. Fan, F. Jiao and H. Qiao, *J. Controlled Release*, 2024, **368**, 355–371.
37 S. J. Klebanoff, *J. Leukocyte Biol.*, 2005, **77**, 598–625.
38 I. Rahman and I. M. Adcock, *Eur. Respir. J.*, 2006, **28**, 219–242.
39 H. S. Park, S. R. Kim and Y. C. Lee, *Respirology*, 2009, **14**, 27–38.
40 Z. Wu, Y. Zheng, J. Sheng, Y. Han, Y. Yang, H. Pan and J. Yao, *Front. Immunol.*, 2022, **13**, 816005.
41 R. N. Zadoks, J. R. Middleton, S. McDougall, J. Katholm and Y. H. Schukken, *J. Mammary Gland Biol. Neoplasia*, 2011, **16**, 357–372.

42 J. Wu, J. Sun, M. Liu, X. Zhang, L. Kong, L. Ma, S. Jiang, X. Liu and W. Ma, *Pharmaceuticals*, 2024, **17**, 1113.
43 S. Wang, Y. Wang, X. Liu, L. Guan, L. Yu and X. Zhang, *J. Ethnopharmacol.*, 2016, **187**, 42–48.
44 W. Lin, B. Gu, Y. Gu, R. Zhao, Y. Huang, R. Fan, W. Rong and Z. Liu, *Int. Immunopharmacol.*, 2024, **138**, 112580.
45 J. Donoso-Quezada, S. Ayala-Mar and J. Gonzalez-Valdez, *Traffic*, 2021, **22**, 204–220.
46 T. Skotland, N. P. Hessvik, K. Sandvig and A. Llorente, *J. Lipid Res.*, 2019, **60**, 9–18.
47 K. Hennigan and E. Lavik, *AAPS J.*, 2023, **25**, 83.
48 A. Oeckinghaus, M. S. Hayden and S. Ghosh, *Nat. Immunol.*, 2011, **12**, 695–708.
49 J. Lai, Y. Liu, C. Liu, M. Qi, R. Liu, X. Zhu, Q. Zhou, Y. Chen, A. Guo and C. Hu, *Inflammation*, 2017, **40**, 1–12.
50 J. Lo, H. Wu, C. Liu, K. Chang, P. Lee, P. Liu, S. Huang, P. Wu, T. Lin, Y. Lai, Y. Chang, Y. Chen, S. Lee, Y. Huang, S. Wang and C. Li, *Int. J. Mol. Sci.*, 2023, **24**, 7300.
51 J. Lo, C. Liu, Y. Li, P. Lee, P. Liu, P. Wu, T. Lin, C. Chen, C. Chiu, Y. Lai, Y. Chang, H. Wu, Y. Chen, Y. Huang, S. Huang, S. Wang and C. Li, *J. Inflamm. Res.*, 2022, **15**, 5347–5359.